

# Photoconductivity in Ac-driven lateral superlattice in the presence of a magnetic field.

**Manuel Torres**

Instituto de Física, Universidad Nacional Autónoma de México, Apartado Postal 20-364, México Distrito Federal 01000, México

E-mail: torres@fisica.unam.mx

**Alejandro Kunold**

Departamento de Ciencias Básicas, Universidad Autónoma Metropolitana Azcapotzalco, Av. San Pablo 180, México Distrito Federal 02200, México

E-mail: akb@correo.azc.uam.mx

## Abstract.

In this work we present a model for the photoconductivity of two-dimensional electron system in a perpendicular homogeneous magnetic field, a weak lateral superlattice, and exposed to millimeter irradiation. The model includes the microwave and Landau contributions in a non-perturbative exact way, the periodic potential is treated perturbatively. The Landau-Floquet states provide a convenient base with respect to which the lattice potential becomes time-dependent, inducing transitions between the Landau-Floquet levels. Based on this formalism, we provide a Kubo-like formula that takes into account the oscillatory Floquet structure of the problem. The total conductivity exhibits strong oscillations, determined by  $\epsilon = \omega/\omega_c$  with  $\omega$  the radiation frequency and  $\omega_c$  the cyclotron frequency. The oscillations follow a pattern with minima centered at  $\omega/\omega_c = j + \frac{1}{2}(l-1) + \delta$ , and maxima centered at  $\omega/\omega_c = j + \frac{1}{2}(l-1) - \delta$ , where  $j = 1, 2, 3, \dots$ ,  $\delta$  is a constant phase shift and  $l$  is the dominant multipole contribution. Negative conductance states develop as the electron mobility and the intensity of the microwave power are increased. It is proposed that, depending on the geometry, negative conductance states or negative resistance states may be observed in lateral superlattices fabricated in *GaAs/AlGaAs* heterostructures.

PACS numbers: 72.40.+w, 73.21.Cd, 75.47.-m, 73.43.-f,

## 1. Introduction.

Photon-assisted tunneling is a well established phenomenon, it is originated from the quasiparticle tunneling in semiconductors irradiated by high frequency fields [1, 2]. It has also been observed in high frequency transport in semiconductor multiquantum well superlattices [3, 4, 5] and nanostructures [6, 7]. Photon assisted tunneling also plays an important role in the development of an intersubband laser [8]. More recently Keay *et al* [9, 10] reported the observation of absolute negative conductance and multiphoton

stimulated emission in sequential resonant tunneling semiconductor superlattices subjected to intense terahertz electric fields. Theoretical studies predicting dynamical localization and absolute negative conductance in semiconductor superlattices subjected to ac electric fields have been known for some time. These studies are based in semiclassical models of electron motion in superlattices in the miniband or coherent tunneling regime [11].

On the other hand, the irradiation with lower frequency fields of two-dimensional electron systems (*2DES*) has remarkable consequences on the transport properties at low magnetic fields. Recently, two experimental groups [12, 13, 14, 15], reported that high mobility *GaAs/Al<sub>x</sub>Ga<sub>1-x</sub>As* heterostructures exposed to radiation from 20 to 150 *GHz* resulted in giant magnetoresistance oscillations, periodic in  $\epsilon = \omega/\omega_c$  with  $\omega$  the radiation frequency and  $\omega_c$  the cyclotron frequency. In the case of high mobility samples the minima of the magnetoresistance oscillations can form zero resistance states (*ZRS*), the series of minima formed at  $\epsilon = j + \delta$ ,  $j = 1, 2, 3, \dots$ ,  $\delta = \frac{1}{2}$  [12, 14], or  $\delta = \frac{1}{4}$  [13, 15]. Two distinct mechanisms for photoconductivity corrections have been proposed: (i) the impurity scattering mechanism, which is caused by the excitation of electrons by the combined effect of photon and impurity scattering [16, 17, 18, 19, 20, 21, 22, 23], and (ii) the distribution function mechanism, which involves redistribution of intra-Landau level population for large inelastic lifetimes [25, 26, 27, 28]. A model for the impurity scattering mechanism was proposed previously by the authors [23, 24], the model includes the microwave and Landau contributions in a non-perturbative exact way, impurity scattering effects are treated perturbatively, the model reproduces various of the experimentally observed features, in particular the fact that negative resistance states (*ZRS*) appear only when the electron mobility exceeds a threshold.

Experimental investigations of lateral superlattices have found interesting commensurability phenomena for the magnetoresistance, both for weak potential modulations [29] and also for strong potential modulations [30]. The observed phenomena can be related to the commensurability of the ratio of the classical cyclotron diameter to the lattice constant, or by particular chaotic trajectories. Lateral superlattices fabricated by cleaving a square grid of cylindrical holes with periodicity  $\approx 100$  to  $120$  *nm* on a *GaAs/AlGaAs* heterostructure have been developed by von Klitzing group [31] in order to provide evidence of the Hofstadter fractal energy spectrum in the quantized Hall conductance.

In the present work we propose that the combined effect of a perpendicular magnetic field plus the irradiation of lateral superlattices can give rise to interesting oscillatory conductance phenomena, with the possible development of negative conductance states (*NCS*). The observation of *NCS* would require a Corbino sample, alternatively negative resistance states (*NRS*) would require a Hall geometry. We consider a *2DES* in the presence of a lateral superlattice and subjected to magnetic and microwave fields. As a first step, it is shown that the dynamics associated with the Landau and radiation contributions can be exactly taken into account. As a second step, the periodic potential is added perturbatively. With respect to the Landau-Floquet states, the periodic

potential acts as a coherent oscillating field which induces transitions between these levels. Based on this formalism, we provide a Kubo-like expression for the conductance that incorporates the oscillatory Floquet structure of the system and the impurity scattering in the usual Born approximation. It is found that  $\sigma_{xx}$  exhibits strong oscillations determined by  $\epsilon = \omega/\omega_c$ . NCS develop for sufficiently high electron mobility and strong microwave power. The model is used to test chirality effects induced by the magnetic field, calculations are carried out for various  $\mathbf{E}$ -field polarization's. Finally, we explore the nonlinear regime in which multiple photon exchange plays an essential role, as well as the current-voltage characteristics of the system.

The paper is organized as follows. In the next section we present the model and the method that allow us to obtain the exact solution of the Landau-microwave system, as well as the perturbative corrections induced by the periodic potential. In section 3 we develop the formulation of the linear response theory valid in arbitrary magnetic and microwave fields. A discussion of relevant numerical calculations is presented in section 4. The last section contains a summary of our main results.

## 2. The Model.

Let us consider the motion of an electron in two dimensions subject to a uniform magnetic field  $\mathbf{B}$  perpendicular to the plane and a constant electric field  $\mathbf{E}_c$ , a periodic potential  $V$  and driven by microwave radiation. On the plane the dynamics is governed by the Schrödinger equation

$$i\hbar\frac{\partial\Psi}{\partial t} = H\Psi = [H_{\{B,\omega\}} + V(\mathbf{r})] \Psi. \quad (1)$$

Here  $H_{\{B,\omega\}}$  is written in terms of the covariant derivative

$$H_{\{B,\omega\}} = \frac{1}{2m^*}\Pi^2, \quad \Pi = \mathbf{p} + e\mathbf{A}, \quad (2)$$

where  $m^*$  is the effective electron mass over the plane that takes into account the effects of the crystalline atomic structure over the charge carriers. The vector potential  $\mathbf{A}$  includes all the contributions of: the magnetic, electric and radiation fields:

$$\mathbf{A} = -\frac{1}{2}\mathbf{r} \times \mathbf{B} + Re \left[ \frac{\epsilon E_\omega}{\omega} \exp\{-i\omega t\} \right] + \mathbf{E}^c t. \quad (3)$$

The superlattice potential  $V(\mathbf{r})$  is decomposed in a Fourier expansion

$$V(\mathbf{r}) = \sum_{mn} V_{mn} \exp \left\{ i2\pi \left( \frac{m x}{a} + \frac{n y}{b} \right) \right\}. \quad (4)$$

We first consider the exact solution of the microwave driven Landau problem, the periodic potential effects are lately added perturbatively. This approximation is justified when the following holds: (i):  $|V|/\hbar\omega_c \ll 1$  and (ii):  $\omega\tau_{tr} \sim \omega_c\tau_{tr} \gg 1$ ;  $\tau_{tr}$  is the transport relaxation time that is estimated using its relation to the electron mobility  $\mu = e\tau_{tr}/m^*$ .

The system posed by  $H_{\{B,\omega\}}$  can be recast as a forced harmonic oscillator, a problem that was solved long time ago by Husimi [32]. Following the formalism developed in references [33, 34], we introduce a canonical transformation to new variables  $Q_\mu, P_\mu$ ;  $\mu = 0, 1, 2$ , according to

$$\begin{aligned} Q_0 &= t, & P_0 &= i\partial_t + e\phi + e\mathbf{r} \cdot \mathbf{E}, \\ \sqrt{eB}Q_1 &= \Pi_y, & \sqrt{eB}P_1 &= \Pi_x, \\ \sqrt{eB}Q_2 &= p_x + eA_x + eBy, & \sqrt{eB}P_2 &= p_y + eA_y - eBx. \end{aligned} \quad (5)$$

It is easily verified that the transformation is indeed canonical, the new variables obey the commutation rules:  $-[Q_0, P_0] = [Q_1, P_1] = [Q_2, P_2] = iB$ ; all other commutators being zero. The inverse transformation gives  $x = l_B(Q_1 - P_2)$ , and  $y = l_B(Q_2 - P_1)$ , where  $l_B = \sqrt{\frac{\hbar}{eB}}$  is the magnetic length. The operators  $(Q_2, P_2)$  can be identified with the generators of the electric-magnetic translation symmetries [35, 36]. Final results are independent of the selected gauge. From the operators in Eq. (5) we construct two pairs of harmonic oscillator-like ladder operators:  $(a_1, a_1^\dagger)$ , and  $(a_2, a_2^\dagger)$  with:

$$a_1 = \frac{1}{\sqrt{2}}(P_1 - iQ_1), \quad a_2 = \frac{1}{\sqrt{2}}(P_2 - iQ_2), \quad (6)$$

obeying:  $[a_1, a_1^\dagger] = [a_2, a_2^\dagger] = 1$ , and  $[a_1, a_2] = [a_1, a_2^\dagger] = 0$ .

It is now possible to find a unitary transformation that exactly diagonalizes  $H_{\{B,\omega\}}$ , it yields

$$W^\dagger H_{\{B,\omega\}} W = \omega_c \left( \frac{1}{2} + a_1^\dagger a_1 \right) \equiv H_0, \quad (7)$$

with the cyclotron frequency  $\omega_c = eB/m^*$  and the  $W(t)$  operator given by

$$W(t) = \exp\{i\eta_1 Q_1\} \exp\{i\xi_1 P_1\} \exp\{i\eta_2 Q_2\} \exp\{i\xi_2 P_2\} \exp\left\{i \int^t \mathcal{L} dt'\right\}, \quad (8)$$

where the functions  $\eta_i(t)$  and  $\xi_i(t)$  represent the solutions to the classical equations of motion that follow from the variation of the Lagrangian

$$\mathcal{L} = \frac{\omega_c}{2} (\eta_1^2 + \zeta_1^2) + \dot{\zeta}_1 \eta_1 + \dot{\zeta}_2 \eta_2 + el_B [E_x (\zeta_1 + \eta_2) + E_y (\eta_1 + \zeta_2)]. \quad (9)$$

It is straightforward to obtain the solutions to the equation of motion, using the expression for the electric field  $\mathbf{E} = -\partial\mathbf{A}/\partial t$  with  $\mathbf{A}$  given in (3). Adding a damping term that takes into account the radiative decay of the quasiparticle, they read

$$\begin{aligned} \eta_1 &= el_B E_\omega \operatorname{Re} \left[ \frac{-i\omega\epsilon_x + \omega_c\epsilon_y}{\omega^2 - \omega_c^2 + i\omega\Gamma_{rad}} e^{i\omega t} \right], & \eta_2 &= el_B E_\omega \operatorname{Re} \left[ \frac{\epsilon_y e^{i\omega t}}{i\omega} \right] + el_B E_y^c t, \\ \zeta_1 &= el_B E_\omega \operatorname{Re} \left[ \frac{\omega_c\epsilon_x + i\omega\epsilon_y}{\omega^2 - \omega_c^2 + i\omega\Gamma_{rad}} e^{i\omega t} \right], & \zeta_2 &= -el_B E_\omega \operatorname{Re} \left[ \frac{\epsilon_x e^{i\omega t}}{i\omega} \right] - el_B E_x^c t. \end{aligned} \quad (10)$$

According to the Floquet theorem the wave function can be written as  $\Psi(t) = \exp(-i\mathcal{E}_\mu t) \phi_\mu(t)$ , where  $\phi_\mu(t)$  is periodic in time, *i.e.*  $\phi_\mu(t + \tau_\omega) = \phi_\mu(t)$ . From Eq. (8) it is noticed that the transformed wave function  $\Psi^W = W\Psi$  contains the phase factor  $\exp\left(i \int^t \mathcal{L} dt'\right)$ . It then follows that the quasienergies and the Floquet modes can

be deduced if we add and subtract to this exponential a term of the form  $\frac{t}{\tau} \int_0^\tau \mathcal{L} dt'$ . Hence, the quasienergies can be readily read off

$$\mathcal{E}_\mu = \mathcal{E}_\mu^{(0)} + \mathcal{E}_{rad}; \quad \mathcal{E}_\mu^{(0)} = \hbar\omega_c \left( \frac{1}{2} + \mu \right), \quad \mathcal{E}_{rad} = \frac{e^2 E_\omega^2 [1 + 2\omega_c \text{Re}(\epsilon_x^* \epsilon_y) / \omega]}{2m^* [(\omega - \omega_c)^2 + \Gamma_{rad}^2]}, \quad (11)$$

here  $\mathcal{E}_\mu^{(0)}$  are the usual Landau energies, and the induced Floquet energy shift is given by the microwave energy  $\mathcal{E}_{rad}$ . The corresponding time-periodic Floquet modes in the  $(P_1, P_2)$  representation are given by

$$\Psi_{\mu,k}(P) = \exp\{-i \sin(2\omega t) F(\omega)\} \phi_\mu(P_1) \delta(P_2 - k), \quad (12)$$

the index  $k$  labels the degeneracy of the Landau-Floquet states, and  $\phi_\mu(P_1)$  is the harmonic oscillator function in the  $P_1$  representation

$$\phi_\mu(P_1) = \langle P_1 | \mu \rangle = \frac{1}{\sqrt{\pi^{1/2} 2^\mu \mu!}} e^{-P_1^2/2} H_\mu(P_1), \quad (13)$$

$H_\mu(P_1)$  is the Hermite polynomial and the function  $F(\omega)$  is given as

$$F(\omega) = \frac{\omega_c}{\omega} \left( \frac{eE_\omega l_B}{\omega^2 - \omega_c^2} \right)^2 \left[ \omega^2 - \omega_c^2 + 2\omega^2 \epsilon_x^2 - 2\omega_c^2 \epsilon_y^2 + \frac{\text{Re}(\epsilon_x^* \epsilon_y)}{\omega \omega_c} (2\omega^4 - \omega^2 \omega_c^2 + \omega_c^4) \right]. \quad (14)$$

Let us now consider the complete Hamiltonian including the contribution from the periodic potential. When the transformation induced by  $W(t)$  is applied, the Schrödinger equation in (1) becomes

$$P_0 \Psi^{(W)} = H_0 \Psi^{(W)} + V_W(t) \Psi^{(W)}, \quad (15)$$

where  $\Psi^{(W)} = W(t)\Psi$  and  $V_W(t) = W(t)V(\mathbf{r})W^{-1}(t)$ . Notice that the periodic potential acquires a time dependence brought by the  $W(t)$  transformation. The problem is now solved in the interaction representation using first order time dependent perturbation theory. In the interaction representation  $\Psi_I^{(W)} = \exp\{iH_0 t\} \Psi^{(W)}$ , and the Schrödinger equation becomes

$$i\partial_t \Psi_I^{(W)} = \{V_W(t)\}_I \Psi_I^{(W)}. \quad (16)$$

The equation has the solution  $\Psi_I^{(W)}(t) = U(t - t_0) \Psi_I^{(W)}(t_0)$ , where  $U(t)$  is the evolution operator. To first order in perturbation theory it is given by the expression

$$U(t) = 1 - i \int_{-\infty}^t dt' [W^\dagger(t') V(\mathbf{r}) W(t')]_I. \quad (17)$$

The interaction is adiabatically turned off as  $t_0 \rightarrow -\infty$ , in which case the asymptotic state is selected as one of the Landau-Floquet eigenvalues of  $H_0$ , *i.e.*  $|\Psi_I^{(W)}(t_0)\rangle \rightarrow |\mu, k\rangle$ . Utilizing the explicit expression for the  $W$  transformation in (8) and after a lengthy calculation the matrix elements of the evolution operator can be worked out as

$$\langle \mu, k | U(t) | \nu, k' \rangle = \delta_{\mu\nu} \delta_{kk'} - \sum_l \sum_{mn} \delta(k - k' + l_B q_n^{(y)}) \frac{e^{il_B q_m^{(x)} (k + l_B q_n^{(y)}) / 2} e^{i(\mathcal{E}_{\mu\nu} + \omega l)t}}{\mathcal{E}_{\mu\nu} + \omega l + \omega_E} C_{\mu\nu, mn}^{(l)}, \quad (18)$$

where  $\omega_E = el_B^2(q_n^{(y)} E_x^c - q_m^{(x)} E_y^c)$ , and the discrete pseudomomenta are given as  $q_m^{(x)} = 2\pi m/a$  and  $q_n^{(y)} = 2\pi n/b$ . The explicit expression for  $C_{\mu\nu, mn}^{(l)}$  is given by

$$C_{\mu,\nu, mn}^{(l)} = \frac{1}{l_B^2} V_{mn} D_{\mu\nu}(\tilde{q}_{mn}) \left( \frac{\Delta_{mn}}{i|\Delta_{mn}|} \right)^l J_l(|\Delta_{mn}|), \quad (19)$$

where  $\tilde{q}_{mn} = il_B(q_m^{(x)} - iq_n^{(y)})/\sqrt{2}$ ,  $J_l$  denote the Legendre polynomials and  $D_{\mu\nu}$  is given in terms of the generalized Laguerre polynomials according to

$$D^{\nu\mu}(\tilde{q}) = \langle \nu | D(\tilde{q}) | \mu \rangle = e^{-\frac{1}{2}|\tilde{q}|^2} \begin{cases} (-\tilde{q}^*)^{\mu-\nu} \sqrt{\frac{\nu!}{\mu!}} L_\nu^{\mu-\nu}(|\tilde{q}|^2), & \mu > \nu, \\ \tilde{q}^{\nu-\mu} \sqrt{\frac{\mu!}{\nu!}} L_\mu^{\nu-\mu}(|\tilde{q}|^2), & \mu < \nu, \end{cases} \quad (20)$$

and

$$\Delta_{mn} = \frac{\omega_c l_B^2 e E_\omega}{\omega(\omega^2 - \omega_c^2 + i\omega\Gamma_{rad})} [\omega(q_m^{(x)} e_x + q_n^{(y)} e_y) + i\omega_c(q_m^{(x)} e_y - q_n^{(y)} e_x)]. \quad (21)$$

Summarizing, the solution to the original Schrödinger equation in Eq. (1) has been achieved by means of three successive transformations:

$$|\Psi_{\mu,k}(t)\rangle = W^\dagger \exp\{-iH_0 t\} U(t-t_0) |\mu, k\rangle, \quad (22)$$

the explicit expressions for  $H_0$ ,  $W$ , and  $U$  are given in Eqs. (7), (8), and (18) respectively.

### 3. Kubo formula for Floquet states.

The usual Kubo formula for the conductivity must be modified in order to include the Floquet dynamics. In the presence of an additional  $DC$  electric field the complete Hamiltonian is  $H_T = H + V_{ext}$ , where  $H$  is the Hamiltonian in Eq. (1) and  $V_{ext} = \frac{1}{m}\mathbf{\Pi} \cdot \mathbf{A}_{ext}$ , with  $\mathbf{A}_{ext} = \frac{\mathbf{E}_0}{\omega} \sin(\Omega t) \exp(-\eta|t|)$ . The static limit is obtained with  $\Omega \rightarrow 0$ , and  $\eta$  represents the rate at which the perturbation is turned on and off. In order to calculate the expectation value of the current density, we need the density matrix  $\rho(t)$  which obeys the von Neumann equation

$$i\hbar \frac{\partial \rho}{\partial t} = [H_T, \rho] = [H + V_{ext}, \rho]. \quad (23)$$

We write to first order  $\rho = \rho_0 + \Delta\rho$ , where the leading term satisfies the equation

$$i\hbar \frac{\partial \rho_0}{\partial t} = [H, \rho_0]. \quad (24)$$

In agreement with Eq. (22),  $\Delta\rho$  is transformed to

$$\tilde{\Delta\rho}(t) = U_I^\dagger(t-t_0) \exp\{iH_0 t\} W(t) \Delta\rho(t) W^\dagger(t) \exp\{-iH_0 t\} U_I(t-t_0). \quad (25)$$

In terms of the transformed density matrix  $\tilde{\Delta\rho}(t)$ , Eq. (23) becomes

$$i\hbar \frac{\partial \tilde{\Delta\rho}}{\partial t} = [\tilde{V}_{ext}, \tilde{\rho}_0], \quad (26)$$

where  $\tilde{V}_{ext}$  and  $\tilde{\rho}_0$  are the external potential and quasi-equilibrium density matrix transformed in the same manner as  $\tilde{\Delta\rho}$  in Eq. (25). The transformed quasi-equilibrium

density matrix is assumed to have the form  $\tilde{\rho}_0 = \sum_{\mu} |\mu\rangle f(\mathcal{E}_{\mu}) \langle \mu|$ , where  $f(\mathcal{E}_{\mu})$  is the usual Fermi function and  $\mathcal{E}_{\mu}$  the Landau-Floquet levels. The argument behind this selection is an adiabatic assumption that the original Hamiltonian  $H$  produces a quasi equilibrium state characterized by the Landau-Floquet eigenvalues [23]. It is straightforward to verify that this selection guarantees that the quasi-equilibrium condition in (24) is verified. Using the results in Eqs. (22) and (25), the expectation value of the density matrix can now be easily obtained from the integration of Eq. (26) with the initial condition  $\Delta\rho(t) \rightarrow 0$  as  $t \rightarrow -\infty$  giving for  $t < 0$

$$\begin{aligned} \langle \Psi_{\mu,k} | \Delta\rho(t) | \Psi_{\nu,k'} \rangle &= \langle \mu, k | \tilde{\Delta}\rho(t) | \nu, k' \rangle \\ &= \frac{e\mathbf{E}_0}{2} \cdot \int_{-\infty}^t \left[ \frac{e^{i(\Omega-i\eta)t'}}{\Omega} f_{\mu\nu} \langle \Psi_{\mu,k} | \mathbf{\Pi}(t') | \Psi_{\nu,k'} \rangle + (\Omega \rightarrow -\Omega) \right], \end{aligned} \quad (27)$$

where the definition  $f_{\mu\nu} = f(\mathcal{E}_{\mu}) - f(\mathcal{E}_{\nu})$  was used. The expectation value for the momentum operator is explicitly computed with the help of Eqs (8), (18), and (22), after a lengthy calculations it yields

$$\langle \Psi_{\mu,k} | \mathbf{\Pi}_i | \Psi_{\nu,k'} \rangle = \sqrt{eB} \sum_l \sum_{mn} \delta(k-k'+l_B q_n^{(y)}) e^{il_B q_m^{(x)}(k+l_B q_n^{(y)}/2)} e^{i(\mathcal{E}_{\mu\nu} + \omega l - i\eta t)} \Delta_{\mu\nu, mn}^{(l)}(j). \quad (28)$$

Here the following definitions were introduced:  $\mathcal{E}_{\mu\nu} = \mathcal{E}_{\mu} - \mathcal{E}_{\nu}$ ,  $a_j = b_j = 1$  if  $j = x$  and  $a_j = -b_j = -i$  if  $j = y$ , and  $\Delta_{\mu\nu, mn}^{(l)}(j)$  is given by

$$\Delta_{\mu\nu, mn}^{(l)}(j) = -\frac{1}{\sqrt{2}} \left[ \frac{a_j \tilde{q}_{mn}^* C_{\mu\nu, mn}^{(l)}}{\mathcal{E}_{\mu\nu} - \omega_c + \omega l - i\eta} + \frac{b_j \tilde{q}_{mn} C_{\mu\nu, mn}^{(l)}}{\mathcal{E}_{\mu\nu} + \omega_c + \omega l - i\eta} \right], \quad (29)$$

the expression for  $C_{\mu\nu, mn}^{(l)}$  are given in (19). Utilizing these results the time integral in Eq. (27) is readily carried out. The current density to first order in the external electric field can now be calculated from  $\langle \mathbf{J}(t, \mathbf{r}) \rangle = Tr [\tilde{\Delta}\rho(t) \tilde{\mathbf{J}}(t)]$ , the resulting expression represents the local density current. Here we are concerned with the macroscopic conductivity tensor that relates the spatially and time averaged current density  $\mathbf{j} = (\tau_{\omega} \mathcal{A})^{-1} \int_0^{\tau_{\omega}} dt \int d^2x \langle \mathbf{J}(t, \mathbf{r}) \rangle$  to the averaged electric field; here  $\tau_{\omega} = 2\pi/\omega$  and  $\mathcal{A}$  is the area of the system (it is understood that  $\mathcal{A} \rightarrow \infty$ ). Assuming that the external electric field points along the  $x$ -axis the macroscopic conductivity can be worked out, results for the dark and microwave induced conductivities are quoted:

$$\sigma_{xi}^D = i \frac{e^2 \omega_c^2}{4\hbar l_B^2} \sum_{\mu\nu} \left\{ \frac{f_{\mu\nu}}{\Omega} \left[ \frac{a_i \mu \delta_{\mu, \nu+1}}{\mathcal{E}_{\mu\nu} + \Omega - i\eta} + \frac{b_i \nu \delta_{\mu, \nu-1}}{\mathcal{E}_{\mu\nu} + \Omega - i\eta} \right] + (\Omega \rightarrow -\Omega) \right\}, \quad (30)$$

$$\sigma_{xi}^{\omega} = \frac{e^2 \omega_c^2}{4\hbar} \sum_{\mu\nu} \left\{ \frac{f_{\mu\nu}}{\Omega} \sum_{mn} \sum_l \frac{\Delta_{\mu\nu, mn}^{(l)}(i) \Delta_{\nu\mu, mn}^{(-l)}(x)}{\mathcal{E}_{\mu\nu} + \omega l + \Omega - i\eta} + (\Omega \rightarrow -\Omega) \right\}. \quad (31)$$

In these expressions the external electric field points along the  $x$ -axis. Hence, setting  $i = x$  or  $i = y$  the longitudinal and Hall conductivities can be selected. The denominators on the R.H.S. of the previous equations can be related to the advanced and retarded Green's functions  $G_{\mu}^{\pm}(\mathcal{E}) = 1/(\mathcal{E} - \mathcal{E}_{\mu} \pm i\eta)$ . To make further progress the real and absorptive parts of the Green's functions are separated taking the limit  $\eta \rightarrow 0$

and using  $\lim_{\eta \rightarrow 0} 1/(\mathcal{E} - i\eta) = P1/\mathcal{E} + i\pi\delta(\mathcal{E})$ , where  $P$  indicates the principal-value integral. As usual the real and imaginary parts contribute to the Hall and longitudinal conductivities respectively. However, the previous expression would present a singular behavior that is an artifact of the  $\eta \rightarrow 0$  limit. This problem is solved by including the disorder broadening effects. A formal procedure requires to calculate the broadening produced by the disorder potential, this calculation has been carried out by Ando [37] and Gerhardtts [38] within the Born Approximation; the density of states for the  $\mu$ -Landau level can be represented by a Gaussian-type form [39]

$$Im G_\mu(\mathcal{E}) = \sqrt{\frac{\pi}{2\Gamma_\mu^2}} \exp [-(\mathcal{E} - \mathcal{E}_\mu)^2/(2\Gamma_\mu^2)], \quad \Gamma_\mu^2 = \frac{2\beta_\mu \hbar^2 \omega_c}{(\pi\tau_{tr})}. \quad (32)$$

The parameter  $\beta_\mu$  in the level width takes into account the difference of the transport scattering time  $\tau_{tr}$  determining the mobility  $\mu$ , from the single-particle lifetime  $\tau_s$ . In the case of short-range scatterers  $\tau_{tr} = \tau_s$  and  $\beta_\mu = 1$ . An expression for  $\beta_\mu$ , suitable for numerical evaluation, that applies for a long-range screened potential is given in reference [23];  $\beta_\mu$  decreases for higher Landau levels; *e.g.*  $\beta_0 \approx 50$ ,  $\beta_{50} \approx 10.5$ .

The static limit with respect to the external field is obtained taking  $\Omega \rightarrow 0$  in Eqs. (30) and (31). In what follows results are presented for the longitudinal microwave induced conductivity, the corresponding dark conductivity expressions as well as the Hall microwave induced conductance are quoted in the appendix. The final result for the microwave induced longitudinal conductance is worked out as

$$\sigma_{xx}^\omega = \frac{e^2}{\pi \hbar l_B^2} \int d\mathcal{E} \sum_{\mu\nu} \sum_l \sum_{mn} Im G_\mu(\mathcal{E}) B^{(l)}(\mathcal{E}, \mathcal{E}_\nu) \left| q_n^{(y)} J_l(|\Delta_{mn}|) V_{mn} D_{\mu\nu}(\tilde{q}_{mn}) \right|^2, \quad (33)$$

where the following functions have been defined

$$B^{(l)}(\mathcal{E}, \mathcal{E}_\nu) = -\frac{d}{d\mathcal{E}_0} \left\{ [f(\mathcal{E} + l\omega + \omega_E + \mathcal{E}_0) - f(\mathcal{E})] Im G_\nu(\mathcal{E} + l\omega + \omega_E + \mathcal{E}_0) \right\} \Big|_{\mathcal{E}_0=0}. \quad (34)$$

#### 4. Results.

The expression in Eq. (33) can be numerically evaluated after the Fourier components  $V_{mn}$  of the periodic potential are specified. We consider two examples, a square lattice potential of the form

$$V(\mathbf{r}) = V_0 \left[ \cos\left(\frac{2\pi x}{a}\right) + \cos\left(\frac{2\pi y}{a}\right) \right], \quad (35)$$

and a hexagonal potential given by [42]

$$V(\mathbf{r}) = V_0 \left[ \cos\left\{\frac{2\pi}{a}\left(\frac{x}{\sqrt{3}} + y\right)\right\} + \cos\left\{\frac{2\pi}{a}\left(\frac{x}{\sqrt{3}} - y\right)\right\} + \cos\left\{\frac{4\pi x}{\sqrt{3}a}\right\} \right]. \quad (36)$$

In our calculations it is assumed that a lateral superlattice is cleaved in ultraclean  $GaAs/Al_xGa_{1-x}As$  sample with high electron mobility,  $\mu \sim 0.5 - 2.5 \times 10^7 cm^2/Vs$ ; the periodic potential has the form given in Eqs. (35,36) with parameters in the range  $a \sim 50 - 200 nm$  and  $V_0 = 1 meV$ . The other parameters of the sample are estimated

as effective electron mass  $m^* = 0.067 m_e$ , fermi energy  $\epsilon_F = 10 meV$ , electron density  $n = 3 \times 10^{11} cm^{-2}$ , and temperature  $T = 1 K$ . For the applied external field we consider magnetic fields in the range  $0.05 - 0.4 Tesla$ , microwave frequencies  $f \sim 10 - 200 GHz$ , and ac-electric field intensity  $|\vec{E}_\omega| \sim 10 - 100 V/cm$  that corresponds to a microwave power characterized by the dimensionless quantity  $\alpha \sim \frac{c\epsilon_0|E_\omega|^2}{m^*\omega^3}$  that varies in the range  $\alpha \sim 0.2 - 1000$ . The relaxation time  $\tau_{tr}$  in Eq. (32) is related with the zero field electron mobility through  $\mu = e\tau_{tr}/m^*$ , and  $\beta_\mu \approx 10.5$ , a value that is justified for large filling factors  $\mu \approx 50$  [23]. A detailed account of the electron dynamics requires to distinguish between various time life's; following reference [41],  $\Gamma_{rad}$  in Eq. (10) is related to the radiative decay width that is interpreted as coherent dipole re-radiation of electromagnetic waves by the oscillating 2D electrons excited by microwaves. Hence, it is given by  $\Gamma_{rad} = 2\pi^2\hbar ne^2/(3\epsilon_0 cm^*)$ , using the values of  $n$  and  $m^*$  given above it yields  $\Gamma_{rad} \sim 2.2 meV$ . In all the examples, except in Fig. 6, we consider the linear regime, the dc-electric field will be included only through the Kubo formula, hence  $\omega_E = 0$  in Eqs. (33), (34). In the case of Fig. 6 the non-linear dc-electric field effects are included using the solution to the classical equations of motion with both ac- and dc-electric fields (10).

Adding the dark and microwave induced conductivities, the total longitudinal  $\sigma_{xx} = \sigma_{xx}^D + \sigma_{xx}^w$ , and Hall  $\sigma_{xy} = \sigma_{xy}^D + \sigma_{xy}^w$  conductivities are obtained. It should be pointed out that the interference between the dark and microwave contributions exactly cancels. The corresponding resistivities are obtained from the expression  $\rho_{xx} = \sigma_{xx}/(\sigma_{xx}^2 + \sigma_{xy}^2)$  and  $\rho_{xy} = \sigma_{xy}/(\sigma_{xx}^2 + \sigma_{xy}^2)$ . The relation  $\sigma_{xy} \gg \sigma_{xx}$  holds in general, hence it follows that  $\rho_{xx} \propto \sigma_{xx}$ , and the longitudinal resistivity follows the same oscillation pattern as that of  $\sigma_{xx}$ .

Fig. 1 displays plots of the total longitudinal conductivity as a function of  $\epsilon = \omega/\omega_c$ . Whereas the dark conductivity presents the expected linear behavior, the total longitudinal conductance shows a strong oscillatory behavior, with distinctive negative conductance states. The periodicity as well as the number of negative conductance regions depends on the intensity of the microwave radiation. In the cases  $\alpha = 2.8$  and  $\alpha = 11$  we observe  $\epsilon$ -periodic oscillations with minima centered at  $\epsilon = 1.1$ ,  $\epsilon = 2.1$ , and  $\epsilon = 3.1$ . Notice that only for the  $\alpha = 11$  case the minima correspond to NCS. A further increase in the microwave intensity ( $\alpha = 44$ ) yields several negative conductance states. The oscillation period is now reduced to  $\frac{1}{2}$ . In general it is observed that  $\sigma_{xx}$  vanishes at  $\omega/\omega_c = j$  for  $j$  integer. The oscillations follow a pattern with minima centered at  $\omega/\omega_c = j + \frac{1}{2}(l - 1) + \delta$ , and maxima centered at  $\omega/\omega_c = j + \frac{1}{2}(l - 1) - \delta$ , where  $j = 1, 2, 3, \dots$ ,  $\delta \approx 1/5$  is a constant phase shift and  $l$  is the dominant multipole that contributes to the conductivity in Eq. (33). For moderate microwave power the  $l = 1$  "one photon" stimulated processes dominate, corresponding to what is observed for  $\alpha = 2.8$  and  $\alpha = 11$ . In the last example ( $\alpha = 44$ ), the results can be interpreted as the results of "two photon" processes ( $l = 2$ ). For small microwave power,  $\sigma_{xx}^w$  is dominated by  $l = 0$  Bessel term in Eq. (33), that is always positive. Negative conductance states arise when the  $l = 1$  and  $l = 0$  terms become comparable:  $J_0(|\Delta|) B^{(0)} \sim J_1(|\Delta|) B^{(1)}$ . A simple analysis show that this condition is fulfilled for  $|\Delta| \sim 0.1$ . Using the result

in Eq. (21), the condition to produce NCS can be estimated as  $|\mathbf{E}_\omega| > E_{th}$  where  $E_{th} \approx 0.1 a \Gamma_{rad} / \sqrt{8} e l_B$ . For the parameter used in Fig. 1,  $E_{th} \approx 10 V/cm$  or  $\alpha_{th} \approx 10$ , in good agreement with the results displayed by the plots.

Next we consider the dependence of  $\sigma_{xx}$  on the lattice parameter  $a$ . Plots of  $\sigma_{xx}$  versus  $\epsilon = \omega/\omega_c$  for various selections of  $a$  are presented in the case of a rectangular (Fig. 2a) and hexagonal lattice (Fig. 2b). A value of  $a_{max}$  for which the oscillation amplitude of  $\sigma_{xx}$  attains its maximum value can be identified in both cases. The precise value depends on the selection of the other parameters. In the present case:  $a_{max} \approx 25 nm$  for the rectangular lattice (Fig. 2a), whereas  $a_{max} \approx 100 nm$  for the hexagonal lattice (Fig. 2b). These plots clearly show that the oscillatory behavior of  $\sigma_{xx}$  and in particular the regions of negative conductivity are governed by the ratio  $\epsilon = \omega/\omega_c$ .

Negative conductivity requires ultra-clean samples, the phenomena appears when the electron mobility exceeds a threshold  $\mu_{th}$ . Fig. 3 displays  $\sigma_{xx}$  v.s.  $\omega/\omega_c$  plots for three selected values of  $\mu$ . For  $\mu \approx 0.5 \times 10^7 cm^2/Vs$  an almost linear behavior  $\sigma_{xx} \propto 1/B$  is clearly depicted. As the electron mobility increases to  $\mu \approx 1.5 \times 10^7 cm^2/Vs$ , the conductivity oscillations are clearly observed; however, negative conductance states only appear when the mobility is increased to  $\mu \approx 2.5 \times 10^7 cm^2/Vs$ . Eqs. (33,34) contain the main ingredients that explain the huge increase observed in the longitudinal conductance (and resistance), when the material is irradiated by microwaves and its critical dependence on the electron mobility. In the standard expression for the Kubo formula there are no Floquet replica contribution, hence  $\omega$  can be set to zero in (34), if that is the case  $B^{(l)}$  becomes proportional to the energy derivative of the Fermi distribution, that in the  $T \rightarrow 0$  limit becomes of the form  $\delta(\mathcal{E} - \mathcal{E}_F)$ , and the conductivity is positive definite depending only on those states lying at the Fermi level. On the other hand, as a result of the periodic structure induced by the microwave radiation,  $B^{(l)}$  contains a second contribution proportional to the derivative of the density of states:  $\frac{d}{d\mathcal{E}} Im G_\nu(\mathcal{E} + l\omega)$ . Due to the oscillatory structure of the density of states, this extra contribution takes both positive and negative values. According to Eq. (32) this second term (as compared to the first one) is proportional to the electron mobility, hence for sufficiently high mobility the new contribution dominates leading to negative conductance states.

The model can be used in order to test chirality effects induced by the magnetic field. Fig. 4 shows the results for different  $\mathbf{E}_\omega$  field polarization's with respect to the current. In (Fig. 4a) it is observed that in the  $\epsilon > 1$  region, the amplitudes of the  $\sigma_{xx}$  oscillation are slightly bigger for transverse polarization as compared to longitudinal polarization. However for  $\epsilon < 1$  a negative conductance region around  $\epsilon = 0.6$  is observed only for longitudinal polarization. A more significant signature is observable for circular polarization. Selecting negative circular polarization (see Fig. 4b), the oscillation amplitudes get the maximum possible value. Instead, for positive circular polarization an important reduction of the oscillatory of amplitudes is observed leading to the total disappearance of the negative conductance states. These results are understood recalling that for negative circular polarization and  $\omega \approx \omega_c$  the electric

field rotates in phase with respect to the electron cyclotron rotation.

The present formalism can also be used in order to explore the non-linear regime in which multiple photon exchange play an essential role. As the microwave radiation intensity is increased, higher multipole ( $l$ ) terms needs to be evaluated. In the explored regime convergent results are obtained including terms up to the  $l = 3$  multipole. In Fig. 5a results are presented for the longitudinal conductivity as a function of the electric field strength ( $E_\omega$ ) of the microwave radiation. Results are displayed for various selections of the magnetic field intensity. In all cases  $\sigma_{xx}$  start from a positive value for  $E_\omega = 0$ . For  $B = 0.067$ , the longitudinal conductivity remains positive for all values of the microwave intensity; instead  $B = 0.055$  the conductivity remains negative above the threshold  $E_\omega \approx 5 V/cm$ . On the other hand for the selections  $B = 0.047$  and  $B = 0.084$ ,  $\sigma_{xx}$  displays an oscillatory behavior, with alternating positive and negative regions.

The non-linear regime with respect to the dc-external field can also be explored within the present formalism. The effect is included using the solution to the classical equations of motion with both ac- and dc-electric fields, Eq.(10). A possible connection between the observed *ZRS* in  $GaAs/Al_xGa_{1-x}As$  heterostructures [12, 13, 14, 15] and the the predicted NRS[16, 17, 18, 19, 20, 21, 22, 23] was put forward by Andreev *etal.* [19], noting that a general analysis of Maxwell equations shows that *NRS* induces an instability that drives the system into a *ZRS*. This mechanism requires the longitudinal current  $j_{xx}$  as a function of  $E_{dc}$  to have a single minimum, the system instability will evolve to the value  $E_{dc}$  in which  $j_{xx}$  cancel. Returning to the irradiated superlattice case, in Fig. 6 it is observed that in general the  $j_{xx}$  vs.  $E_{dc}$  plot has an oscillatory behavior, with more than one minima. Hence the conditions of the Andreev mechanism do not apply. Consequently, negative conductance states may be probably observed in 2-dimensional lateral superlattices, when exposed to both magnetic and microwave fields.

## 5. Conclusions.

We have considered a model to describe the conductivity of an electron in a 2-dimensional lateral superlattice subjected to both a magnetic field and microwave radiation. We presented a thorough discussion of the method to take into account the Landau and microwave contributions in a non-perturbative exact way, the periodic potential effects are treated perturbatively. The method exploits the symmetries of the problem: the exact solution of the Landau-microwave dynamics (7) is obtained in terms of the electric-magnetic generators (5) as well as the solutions to the classical equations of motion (9). The spectrum and Floquet modes are explicitly worked out. In our model, the Landau-Floquet states act coherently with respect to the oscillating field of the superlattice potential, that in turn induces transitions between these levels. Based on this formalism, a Kubo-like formula is provided, it takes into account the oscillatory Floquet structure of the problem.

It is found that  $\sigma_{xx}$  exhibits strong oscillations determined by  $\epsilon = \omega/\omega_c$ . The oscillations follow a pattern with minima centered at  $\omega/\omega_c = j + \frac{1}{2}(l - 1) + \delta$ , and

maxima centered at  $\omega/\omega_c = j + \frac{1}{2}(l - 1) - \delta$ , where  $j = 1, 2, 3, \dots$ ,  $\delta \approx 1/5$  is a constant phase shift and  $l$  is the dominant multipole contribution. NCS develop for sufficiently strong microwave power (Fig. 1) and high electron mobility (Fig. 3). According to the Eqs. (33) and (34) the longitudinal photoconductivity contains a new contribution proportional to the derivative of the density of states:  $\frac{d}{d\mathcal{E}} \text{Im} G_\nu(\mathcal{E} + l\omega)$ . Due to the oscillatory structure of the density of states this extra contribution takes both positive and negative values. This term is proportional to the electron mobility, hence for sufficiently high mobility the new contribution dominates leading to negative conductivity states.

An interesting prediction of the present model is related to polarization effects. While the results for the cases of linear transverse or longitudinal polarization's show small differences, the selection of circular polarized radiation leads to significant signatures. The maximum possible value for the oscillation amplitudes of  $\sigma_{xx}$  appears for negative circular polarization. Instead, positive circular polarization yields an important reduction on the oscillation amplitudes and the total disappearance of the NCS. This result can be understood, if one recalls that for negative circular polarization and  $\omega \approx \omega_c$  the electric field rotates in phase with respect to the electron cyclotron rotation.

In conclusion, it is proposed that the combined effect of a perpendicular magnetic field plus the irradiation of lateral superlattices can give rise to interesting oscillatory conductance phenomena, with the possible development of negative conductance states (NCS). One should stress that according to our results, the production of NCS requires ultra-clean samples with electron mobilities of order  $\mu \approx 2.5 \times 10^7 \text{ cm}^2/\text{Vs}$  (see Fig. 3). The electron mobilities in the lateral superlattices fabricated so far [31] are  $\mu \approx 2.5 \times 10^6 \text{ cm}^2/\text{Vs}$ , consequently an increase on the electron mobilities of these kind of experimental setups by an order of magnitude would be required in order to observe NCS.

## Acknowledgments

We acknowledge the partial financial support endowed by CONACyT through grants No. 42026-F and G32736-E, and UNAM project No. IN113305.

## Appendix: Dark and Hall conductivities.

In section 3 the method to obtain the final expression for the microwave induced conductance Eq. (33) was explained in detail. Working along a similar procedure the expression for the remaining conductivities are worked from equations (30) and (31). First we quote the longitudinal dark conductance

$$\sigma_{xx}^D = \frac{e^2 \omega_c^2}{\pi \hbar} \sum_{\mu} \mu \int d\mathcal{E} \text{Im} G_{\mu}(\mathcal{E}) \frac{df}{d\mathcal{E}} \text{Im} G_{\mu}(\mathcal{E} + \omega_c) , \quad (.1)$$

whereas the dark Hall conductance is given by

$$\sigma_{xy}^D = \frac{e^2 \omega_c^2}{\pi \hbar} \sum_{\mu} \mu \int d\mathcal{E} \operatorname{Im} G_{\mu}(\mathcal{E}) [f(\mathcal{E}_{\mu} - \omega_c) - f(\mathcal{E})] P \frac{1}{(\mathcal{E} - \mathcal{E}_{\mu} + \omega_c)^2}, \quad (.2)$$

where  $P$  indicates the principal-value integral. The final result for the microwave assisted longitudinal conductivity was quoted in Eq. (33). Following a similar procedure the microwave assisted Hal conductivity is calculated to give

$$\sigma_{xy}^{\omega} = \frac{e^2 \omega_c^2}{\pi \hbar} \int d\mathcal{E} \sum_{\mu\nu} \sum_l \sum_{mn} \operatorname{Im} G_{\mu}(\mathcal{E}) [f(\mathcal{E}_{\nu}) - f(\mathcal{E})] T_{mn} \left| \tilde{J}_l (|\Delta_{mn}|) V_{mn} D_{\mu\nu}(\tilde{q}_{mn}) \right|^2, \quad (.3)$$

were the function  $T_{mn}$  is defined as

$$T_{mn} = \omega_c^3 \frac{(q_m^{(x)})^2 + (q_n^{(y)})^2}{(\mathcal{E} + \omega l - \mathcal{E}_{\nu}) |(\mathcal{E} + \omega l - \mathcal{E}_{\nu})^2 - \omega_c^2|^2}. \quad (.4)$$

## References

- [1] P. K. Tien, J. P. Gordon, *Phys. Rev.* **129** (1993) 647.
- [2] G. Bastard, J. A. Brown, R. Ferreira, “*Solid State Physics: Semiconductor Heterostructures and Nanostructures, edited by H. Ehrenreich and D. Turnbull*”, (Academic Press, San Diego, 1994), Vol. 44, p. 325.
- [3] P. S. S. Guimaraes, B. J. Keay, J. P. Kaminsky, S. J. Allen Jr., P. F. Hopkins, A. C. Gossard, L. T. Florez, J. P. Harbison, *Phys. Rev. Lett.* **70** (1993) 3792.
- [4] B. J. Keay, P. S. S. Guimaraes, J. P. Kaminsky, S. J. Allen Jr., P. F. Hopkins, A. C. Gossard, L. T. Florez, J. P. Harbison, *Surf. Sci.* **305** (1994) 385.
- [5] B. J. Keay, S. J. Allen Jr., J. Galán, J. P. Kaminsky, K. L. Campmann, A. C. Gossard, U. Bhattacharya, M. J. W. Rodwell, *Phys. Rev. Lett.* **75** (1995) 4098.
- [6] S. Verghese, R. A. Wyss, Th. Schäpers, A. Förster, M.J. Rooks, Q. Hu, *Phys. Rev. B* **52** (1995) 14834.
- [7] L. P. Kouwenhoven, S. Jauhar, J. Orenstein, P. L. McEuen, *Phys. Rev. Lett.* **73** (1994) 3443.
- [8] J. Faist, F. Capasso, D. L. Sivco, C. Sirtori, A. L. Hutchinson, A. Y. Cho, *Science* **264** (1994) 553.
- [9] B. J. Keay, S. Zeuner, S. J. Allen Jr., K. D. Maranowski, A. C. Gossard, U. Bhattacharya, M. J. W. Rodwell, *Phys. Rev. Lett.* **75** (1995) 4102.
- [10] S. Zeuner, B. J. Keay, S. J. Allen Jr., K. D. Maranowski, A. C. Gossard, U. Bhattacharya, M. J. W. Rodwell, *Phys. Rev. B* **53** (1996) R1717.
- [11] For a review see: G. Platero, R. Aguado, *Phys. Reports.* **395** (2004) 1.
- [12] M. A. Zudov, R. R. Du, J. A. Simmons, J. L. Reno, *Phys. Rev. B* **64** (2001) 201311(R).
- [13] R. G. Mani, J. H. Smet, K. von klitzing, V. Narayanamurti, W.b. Johnson, Umansky, *Nature* **420** (2002) 646; *Phys. Rev. Lett* **92** (2004) 146801.
- [14] M. A. Zudov, R. R. Du, L. N. Pfeiffer, K. W. West, *Phys. Rev. Lett* **90** (2003) 046807.
- [15] R. G. Mani, *Physica E* **22** (2004) 1.
- [16] V. I. Ryzhii, *Sov. Phys. Solid State* **11** (1970) 2078.
- [17] V. I. Ryzhii, R. Suris, *J Phys. Cond. Matt.* **15** (2003) 6855.
- [18] A. C. Durst, S. Sachdev, N. Read, S. M. Girvin, *Phys. Rev. Lett.* **91** (2003) 086803.
- [19] A. V. Andreev, I. L. Aleiner, A. J. Millis, *Phys. Rev. Lett.* **91** (2003) 056803.
- [20] J. Shi, X. C. Xie, *Phys. Rev. Lett.* **91** (2003) 086801.
- [21] X. L. lei, S. Y. Liu, *Phys. Rev. Lett.* **91** (2003) 226805.
- [22] M. G. Vavilov, I. L. Aleiner, *Phys. Rev. B* **69** (2004) 035303.
- [23] M. Torres, A. Kunold, *Phys. Rev. B* **71** (2005) 115313-1.

- [24] M. Torres, A. Kunold, *Phys. Stat. Sol. b* **71** (2005) 1192.
- [25] S. I. Dorozhkin, *JETP. Letters.* **77** (2003) 577.
- [26] I. A. Dmitriev, A. D. Mirlin, D. G. Polyakov, *Phys. Rev. Lett.* **91** (2003) 226802.
- [27] I. A. Dmitriev, M. G. Vavilov, I. L. Aleiner, A. D. Mirlin, D. G. Polyakov, *Phys. Rev. B* **71** (2005) 115316.
- [28] J. P. Robinson, M. P. Kennett, , N. R. Cooper, V. I. Fal'ko, *Phys. Rev. Lett.* **93** (2004) 036804
- [29] D. Weiss, K. v. Klitzing, K. Ploog, G. Weimann, *Europhys. Lett.* **8** (1989) 179; R. W. Winkler, J. P. Kotthaus, K. Ploog, *Phys. Rev. Lett.* **62** (1989) 1177; D. Weiss, M. L. Roukes, A. Menschig, P. Grambow, K. v. Klitzing, G. Weimann, *Phys. Rev. Lett.* . **66** (1991) 2790.
- [30] For a review see R. Schuster, K. Ensslin, *Adv. Solid State Phys.* **34** (1994) 195.
- [31] C. Albrecht, J. H. Smet, K. v. Klitzing, D. Weiss, V. Umansky, H. Schweizer , *Phys. Rev. Lett.* **86** (2001) 147.
- [32] K. Husimi, *Prog. Theor. Phys.* **9** (1953) 381.
- [33] A. Kunold, M. Torres, *Phys. Rev. B* **61** (2000) 9879.
- [34] M. Torres, A. Kunold, *Phys. Lett. A* **323** (2004) 2890.
- [35] N. Ashby and S.C. Miller, *Phys. Rev. B* **139** (1965) A428.
- [36] A. Kunold, M. Torres, *Annals of Physics* **315** (2005) 532.
- [37] T. Ando, Y. Uemura, *J. Phys. Soc. Japan.* **36** (1974) 959.
- [38] R. R. Gerhardts, *Z. Phys. B* **21** (1975) 275; *Ibid.* **21** (1975) 285.
- [39] T. Ando, A. B. Fowler, F. Stern, *Rev. Mod. Phys.* **54** (1982) 437.
- [40] T. Dittrich, P. hanggi, G.L. Ingold, B. Kramer, G. Schon, W. Zwerger, “*Quantum transport and dissipation*”, Wiley-VCH (1998).
- [41] S. A. Mikhailov, *Phys. Rev. B* **70** (2004) 165311.
- [42] F. H. Claro, G. H. Wannier, *Phys. Rev. B* **19** (1979) 6068.

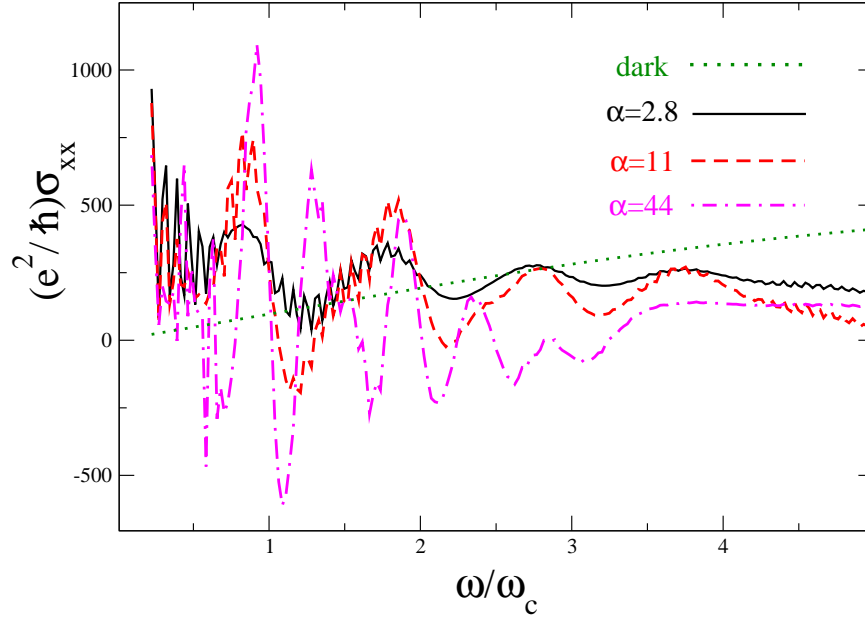


**Figure 1.** Longitudinal conductivity as a function  $\epsilon = \omega/\omega_c$  for four values of the microwave power intensity. The dotted line corresponds to the dark case (without microwave radiation) the other plots are for:  $\alpha = 2.8$  continuous line;  $\alpha = 11$  dashed line; and  $\alpha = 44$  dashed-dotted line. The microwave polarization is linear transverse (with respect to the current), the frequency  $f = 25 \text{ GHz}$  and the power is characterized by the dimensionless parameter  $\alpha = c\epsilon_0|E_\omega|^2/(m^*\omega^3)$ . The potential corresponds to a square lattice, Eq. (35), with  $a = 100 \text{ nm}$ , and  $V_0 = 1 \text{ meV}$ . The other parameters are selected as follows:  $m^* = 0.067 m_e$ ,  $\mu \approx 2.5 \times 10^7 \text{ cm}^2/\text{Vs}$ ,  $\epsilon_F = 10 \text{ meV}$ ,  $T = 1 \text{ K}$ .

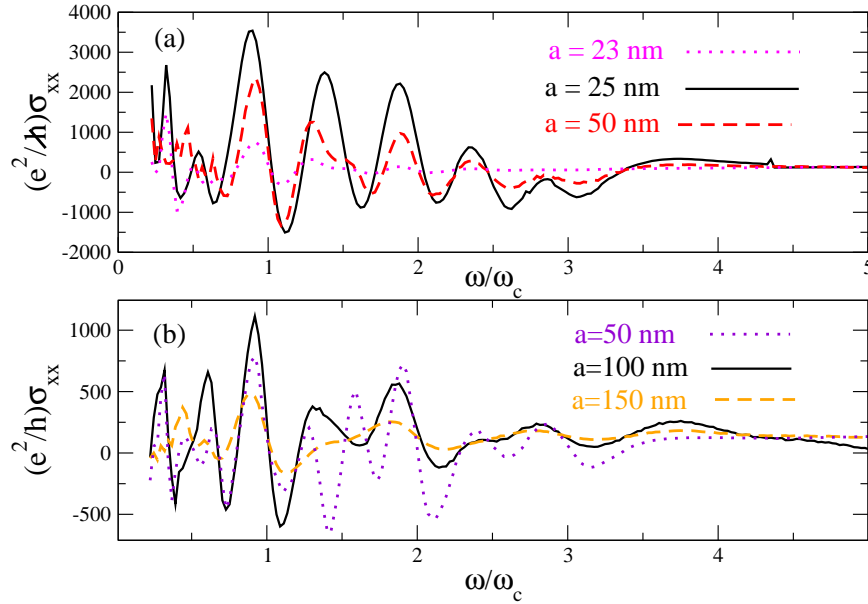


**Figure 2.** Longitudinal conductivity as a function of  $\epsilon = \omega/\omega_c$  for: (a) Square lattice, Eq. (35):  $a = 23$  nm dotted line,  $a = 25$  nm continuous line, and  $a = 50$  nm dashed line. (b) Hexagonal lattice, Eq. (36):  $a = 50$  nm dotted line,  $a = 100$  nm continuous line, and  $a = 150$  nm dashed-dotted line. The microwave power is given by  $\alpha = 11$ , corresponding to an ac-electric field intensity of  $E_\omega = 10$  V/cm. The other parameters have the same values as in Fig. 1.

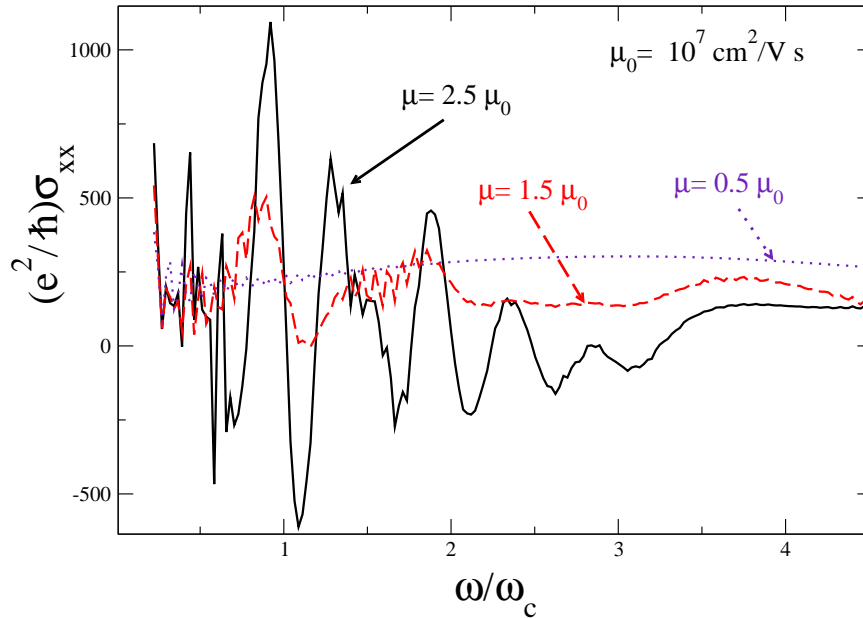


**Figure 3.** Longitudinal conductivity as a function  $\epsilon = \omega/\omega_c$  for three values of the electron mobility:  $\mu = 0.5 \times 10^7$  cm<sup>2</sup>/V s dotted line,  $\mu = 1.5 \times 10^7$  cm<sup>2</sup>/V s dashed line, and  $\mu = 2.5 \times 10^7$  cm<sup>2</sup>/V s continuous line. The microwave power is given by  $\alpha = 11$ , the other parameters have the same values as in Fig. 1.

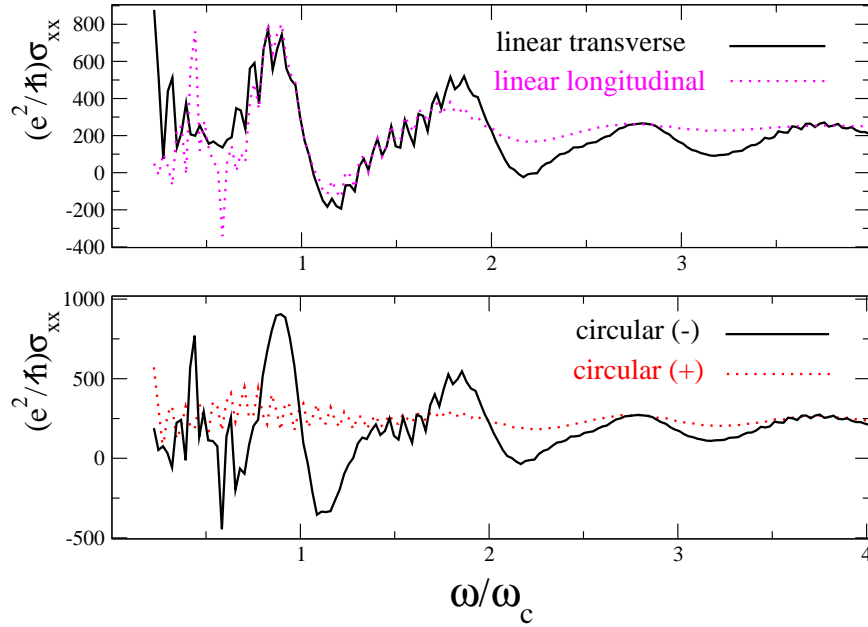


**Figure 4.** Longitudinal conductance *vs.*  $\epsilon = \omega/\omega_c$  for various microwave  $E_\omega$ -field polarization's with respect to the current. In figure (a) the continuous and dotted lines correspond to linear transverse and longitudinal polarization's respectively. Figure (b) shows results for circular polarization's: left-hand (continuous line) and right-hand (dotted line).  $\alpha = 11$  and the values of the other parameters are the same as in figure Fig. 1

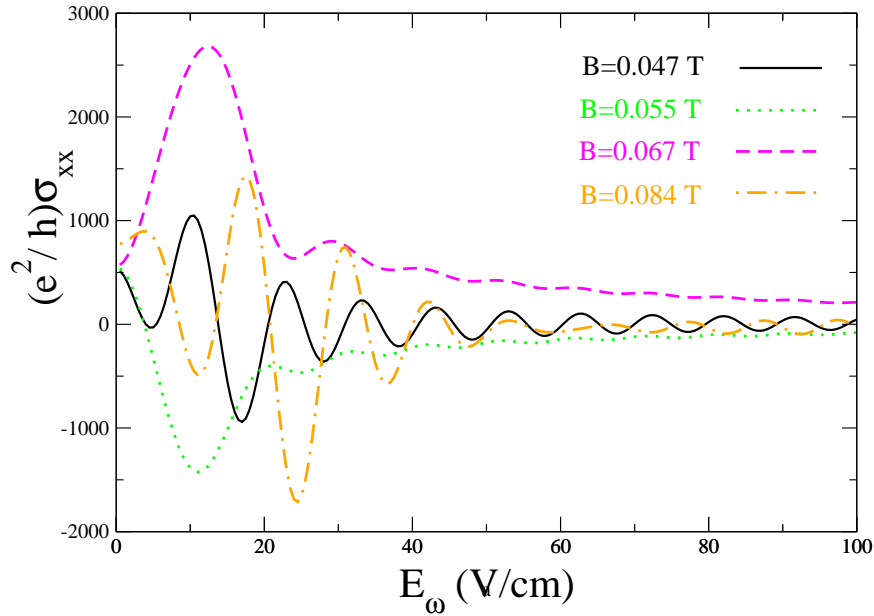


**Figure 5.** Longitudinal conductivity as a function of the microwave ac-electric field for four values of the magnetic field intensity:  $B = 0.047$  T continuous line,  $B = 0.055$  T dotted line,  $B = 0.067$  T dashed line, and  $B = 0.084$  T dashed-dotted line. The other parameters have the same values as in Fig. 1

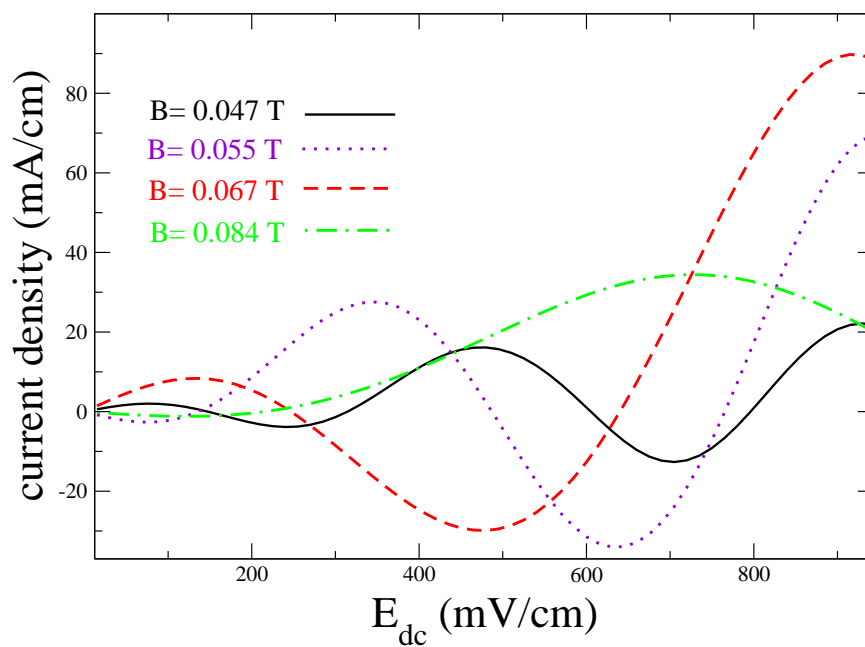


**Figure 6.** Current-voltage characteristics for the irradiated sample for four values of the magnetic field intensity:  $B = 0.047$  T continuous line,  $B = 0.055$  T dotted line,  $B = 0.067$  T dashed line, and  $B = 0.084$  T dashed-dotted line. The other parameters have the same values as in Fig. 1